

## Supporting Information

### Colloidal Synthesis of Heterostructured $\text{CuCo}_2\text{S}_4/\text{g-C}_3\text{N}_4/\text{In}_2\text{S}_3$ Nanocomposite for Photocatalytic Hydrogen Evolution

Amit Gautam,<sup>ab</sup> Saddam Sk,<sup>ab</sup> Aparna Jamma,<sup>ab</sup> B Moses Abraham,<sup>c</sup> Mohsen Ahmadipour<sup>d</sup> and Ujjwal Pal<sup>\*ab</sup>

---

*a.* Department of Energy & Environmental Engineering, CSIR-Indian Institute of Chemical Technology, Hyderabad-500007, India.

*b.* Academy of Scientific and Innovative Research (AcSIR), Ghaziabad-201002, India.

*c.* Department of Chemical Engineering, Indian Institute of Technology Kanpur, Kanpur-208016, India.

*d.* Institute of Microengineering and Nanoelectronics, Universiti Kebangsaan Malaysia, 43600 Bangi, Selangor, Malaysia.

---

\* E-mail: upal03@gmail.com, ujjwalpal@iict.res.in

## Characterization

The structural phase analysis of the as-synthesized photocatalysts was performed by using Powder X-ray diffraction patterns (XRD) on a Bruker AXS diffractometer (D8 advance) at a generator voltage of 40 kV and current of 30 mA using Cu-K $\alpha_1$  irradiation ( $\lambda = 1.5406 \text{ \AA}$ ). The sample was scanned in the range of  $2\theta = 10\text{-}80^\circ$  with a scan rate of 1 s/step. X-ray photoelectron spectroscopy (XPS) was performed via a Kratos (axis 165) analytical instrument with Mg K $\alpha$  irradiation. About  $10^{-9}$  Torr pressure was maintained in the spectrometer. The Field emission scanning electron microscopy (FESEM) images of sample were taken by using JEOL JSM 7610F. Transmission electron microscopy (TEM) image of the representative photocatalysts was obtained by using a JEOL 2010EX TEM instrument equipped with the high-resolution style objective-lens pole piece at an acceleration voltage of 200 kV fitted with a CCD camera. All TEM samples were prepared by depositing a drop of diluted suspensions in acetone on a carbon coated copper grid and allowed to dry naturally. FT-IR spectroscopy was used to characterize the surface feature of the particles. The optical properties were characterized by using UV-Vis diffuse reflectance spectroscopy (DRS) Perkin Elmer Lambda 750 instrument using BaSO $_4$  as a reference. The sample has been placed in the sample holder for the measurement and the light is allowed to pass through the sample which leads to the absorption of the light and the light transmitted by the sample has been recorded. The Photoluminescence (PL) spectra were recorded using a Fluorolog-3 spectrofluorometer (Spex model, JobinYvon) at their respective excitation ( $\lambda_{\text{ex}}$ ) wavelength.

## Computational details

The Perdew-Burke-Ernzerhof (PBE)<sup>1</sup> exchange-correlation functional with a generalized gradient approximation to describe the exchange-correlation energy and the projector augmented-wave (PAW) potentials<sup>2</sup> to express the ion-electron interactions were employed to perform plane wave-based Vienna ab initio simulation package (VASP)<sup>3</sup> calculations within the framework of density functional theory (DFT). The structural relaxation was performed on its atoms and cell parameters until the total energy was nearly within  $10^{-5}$  eV. A Monkhorst-Pack grid<sup>4</sup> with a  $\Gamma$ -centered sampling was used to sample the k-space. The conjugate gradient algorithm was used to perform geometry optimization for electronic minimizations, ensuring that the atomic forces on each atom in the relaxed structures were below  $0.01 \text{ eV\AA}^{-1}$ . To prevent

potential interaction between periodic images, a vacuum layer of around 15 Å is applied along the z-direction. The expansion of the plane-wave basis set was achieved by setting a kinetic energy cutoff of 500 eV. The DFT-D3 approach,<sup>5</sup> which is a popular dispersion correction method, was employed to accurately account for van der Waals interactions. The use of standard GGA-PBE based DFT for electronic property calculations typically contains reliability issues, leading us to adopt the screened hybrid HSE06 function.<sup>6, 7</sup> This function offers superior accuracy in predicting electronic properties by integrating Hartree-Fock and semilocal GGA theories. To construct g-C<sub>3</sub>N<sub>4</sub>/CuCoS<sub>4</sub> binary heterostructure and the subsequent g-C<sub>3</sub>N<sub>4</sub>/CuCoS<sub>4</sub>/In<sub>2</sub>S<sub>3</sub> ternary heterostructure, we utilized g-C<sub>3</sub>N<sub>4</sub> as the substrate material.

### **Electrochemical measurements**

All the electrochemical measurements have been carried out in a three-electrode system using a potentiostat (CH Instruments, CHI 6005E, USA) with an aqueous 0.25 M Na<sub>2</sub>SO<sub>4</sub> electrolytic solution using Ag/AgCl saturated with KCl as reference electrode, Pt wire as a counter electrode, and sample loaded modified ITO film as a working electrode. The sample loading over the ITO film with a surface area of 2\*2 cm<sup>2</sup> has been carried out by the dispersion of 5 mg of the sample into 200 µL ethanol and 30 µL of Nafion through ultrasonication and drop cast over the ITO film and dried at RT..

### **Photocatalytic hydrogen generation experiment**

Photocatalytic hydrogen production was carried out as follows: The photocatalytic hydrogen production experiments were performed in a 100 mL Quartz photoreactor at room temperature and atmospheric pressure, and the outlet of the flask was sealed with a silicone rubber septum. In a typical photocatalytic experiment, 10 mg of catalyst was dispersed by constant stirring in 30 mL DI H<sub>2</sub>O containing 0.35 M Na<sub>2</sub>S and 0.25 M Na<sub>2</sub>SO<sub>3</sub> as the sacrificial electron donor. Before irradiation, the system was bubbled with nitrogen for 30 min to remove the oxygen and ensured that the reaction system was under an anaerobic condition. A 300 W Xe arc lamp (Newport Co., Ltd., USA) with a cut-off filter ( $\lambda \geq 420$  nm), which was positioned 10 cm away from the reactor, was used as a light source to trigger the photocatalytic reaction. The evolved gas produced from the upper space above the solution in the reactor was periodically analysed by sampling for each hour using gas chromatography (Perkin Elmer Clarus 590 GC containing

molecular Sieve 5Å column) with thermal conductivity detector (TCD) using N<sub>2</sub> as carrier gas at periodic time intervals.

### Apparent quantum yield (AQY) calculation

The apparent quantum yield (AQY) has been measured under the same photoreaction conditions. An optical power/energy meter (Newport, Model: 842-PE) was used to determination of the number of incident photons ( $N_{\text{photons}}$ ). The values of  $N_{\text{photons}}$  and AQY % were calculated using a band-pass filter of 420 nm using the following equations:<sup>8,9</sup>

$$N_{\text{photon}} = \frac{P\lambda t}{hc}$$

Here, P represents the power of the light ( $0.16 \text{ W cm}^{-2} = 0.16 \text{ J s}^{-1} \text{ cm}^{-2}$ ) in an area of  $11.17 \text{ cm}^2$ ,  $\lambda$  is the wavelength of the light (420 nm), t is the duration of irradiation (4 h), h is the Planck's constant ( $6.626 \times 10^{-34} \text{ J s}$ ) and c is the velocity of light ( $3 \times 10^8 \text{ m s}^{-1}$ ).

$$N_{\text{photon}} = \frac{0.16 \times 11.17 \times 420 \times 10^{-9} \times 4 \times 3600}{6.626 \times 10^{-34} \times 3 \times 10^8} = 4.92 \times 10^{22}$$
$$\text{AQY \%} = \frac{2 \times \text{numbers of evolved } H_2 \text{ molecule}}{\text{numbers of incident photons } (N_{\text{photon}})} \times 100$$

**Table S1: Photocatalytic H<sub>2</sub> generation efficiency of the composites under visible light irradiation for 4 hrs.**

photocatalysts	H <sub>2</sub> evolution Rate (mmol g <sup>-1</sup> h <sup>-1</sup> )	AQY (%)
CuCo <sub>2</sub> S <sub>4</sub>	1.32	3.20
CuCo <sub>2</sub> S <sub>4</sub> /g-C <sub>3</sub> N <sub>4</sub> (2 wt%)	4.58	11.09
CuCo <sub>2</sub> S <sub>4</sub> /g-C <sub>3</sub> N <sub>4</sub> (4 wt%)	5.19	12.55
CuCo <sub>2</sub> S <sub>4</sub> /g-C <sub>3</sub> N <sub>4</sub> (6 wt%)	4.86	11.76
CuCo <sub>2</sub> S <sub>4</sub> /g-C <sub>3</sub> N <sub>4</sub> (8 wt%)	4.32	10.46
CuCo <sub>2</sub> S <sub>4</sub> /g-C <sub>3</sub> N <sub>4</sub> (4 wt%)/In <sub>2</sub> S <sub>3</sub> (3 wt%)	6.04	14.61
CuCo <sub>2</sub> S <sub>4</sub> /g-C <sub>3</sub> N <sub>4</sub> (4 wt%)/In <sub>2</sub> S <sub>3</sub> (5 wt%)	11.66	28.22
CuCo <sub>2</sub> S <sub>4</sub> /g-C <sub>3</sub> N <sub>4</sub> (4 wt%)/In <sub>2</sub> S <sub>3</sub> (10 wt%)	7.23	17.49
CuCo <sub>2</sub> S <sub>4</sub> /g-C <sub>3</sub> N <sub>4</sub> (4 wt%)/In <sub>2</sub> S <sub>3</sub> (20 wt%)	7.22	17.47
CuCo <sub>2</sub> S <sub>4</sub> /In <sub>2</sub> S <sub>3</sub> (5 wt%)	3.92	9.49
In <sub>2</sub> S <sub>3</sub> /g-C <sub>3</sub> N <sub>4</sub> (4 wt%)	2.87	6.95
g-C <sub>3</sub> N <sub>4</sub>	0.23	0.56
In <sub>2</sub> S <sub>3</sub>	0.45	1.10

**Table S2: Comparative table of photocatalytic hydrogen evolution activity.**

Photocatalyst	Light source	SED	H <sub>2</sub> activity	Ref.
ZnFe <sub>2</sub> O <sub>4</sub> /CdS Nanorods	400W Hg lamp	0.175M Na <sub>2</sub> S 0.125M Na <sub>2</sub> SO <sub>3</sub>	2.44 mmolg <sup>-1</sup> h <sup>-1</sup>	<sup>10</sup>
Mn <sub>0.8</sub> Cd <sub>0.2</sub> S/g-C <sub>3</sub> N <sub>4</sub>	300W Xe lamp (λ ≥ 420 nm)	Na <sub>2</sub> S/Na <sub>2</sub> SO <sub>3</sub>	4 mmolg <sup>-1</sup> h <sup>-1</sup>	<sup>11</sup>
CoS <sub>x</sub> /Mn <sub>0.5</sub> Cd <sub>0.5</sub> S	300W Xe lamp (λ ≥ 420 nm)	Na <sub>2</sub> S/Na <sub>2</sub> SO <sub>3</sub>	8.6 mmolg <sup>-1</sup> h <sup>-1</sup>	<sup>12</sup>
Ni <sub>2</sub> O <sub>3</sub> /Mn <sub>0.2</sub> Cd <sub>0.8</sub> S/Cu <sub>3</sub> P @Cu <sub>2</sub> S	300W Xe lamp (λ ≥ 400 nm)	Na <sub>2</sub> S/Na <sub>2</sub> SO <sub>3</sub>	9.2 mmolg <sup>-1</sup> h <sup>-1</sup>	<sup>13</sup>
CdS/MoS <sub>2</sub> /rGO	300W Xe lamp (λ ≥ 420 nm)	Na <sub>2</sub> S/Na <sub>2</sub> SO <sub>3</sub>	9.000 mmolg <sup>-1</sup> h <sup>-1</sup>	<sup>14</sup>
CdS/MoS <sub>2</sub>	300W Xe lamp (λ ≥ 420 nm)	Lactic Acid	10.2 mmolg <sup>-1</sup> h <sup>-1</sup>	<sup>15</sup>
<b>CuCo<sub>2</sub>S<sub>4</sub>/g-C<sub>3</sub>N<sub>4</sub>/In<sub>2</sub>S<sub>3</sub></b>	<b>300W Xe lamp</b> <b>(λ ≥ 420 nm)</b>	<b>Na<sub>2</sub>S/Na<sub>2</sub>SO<sub>3</sub></b>	<b>11.66 mmolg<sup>-1</sup>h<sup>-1</sup></b>	<b>This work</b>

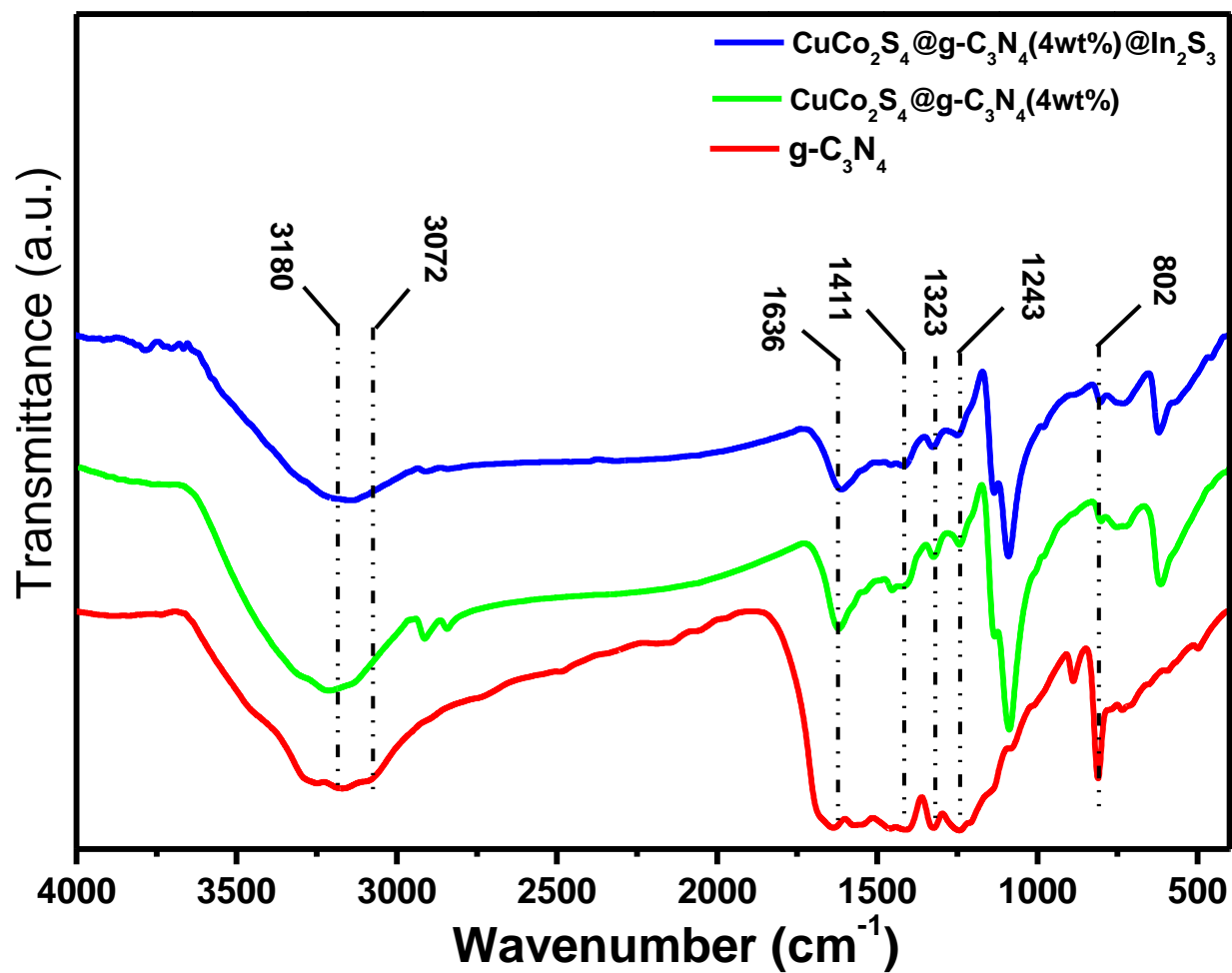


**Figure S1.** FTIR spectra of  $\text{g-C}_3\text{N}_4$ ,  $\text{CuCo}_2\text{S}_4/\text{g-C}_3\text{N}_4$  and  $\text{CuCo}_2\text{S}_4/\text{g-C}_3\text{N}_4/\text{In}_2\text{S}_3$ .

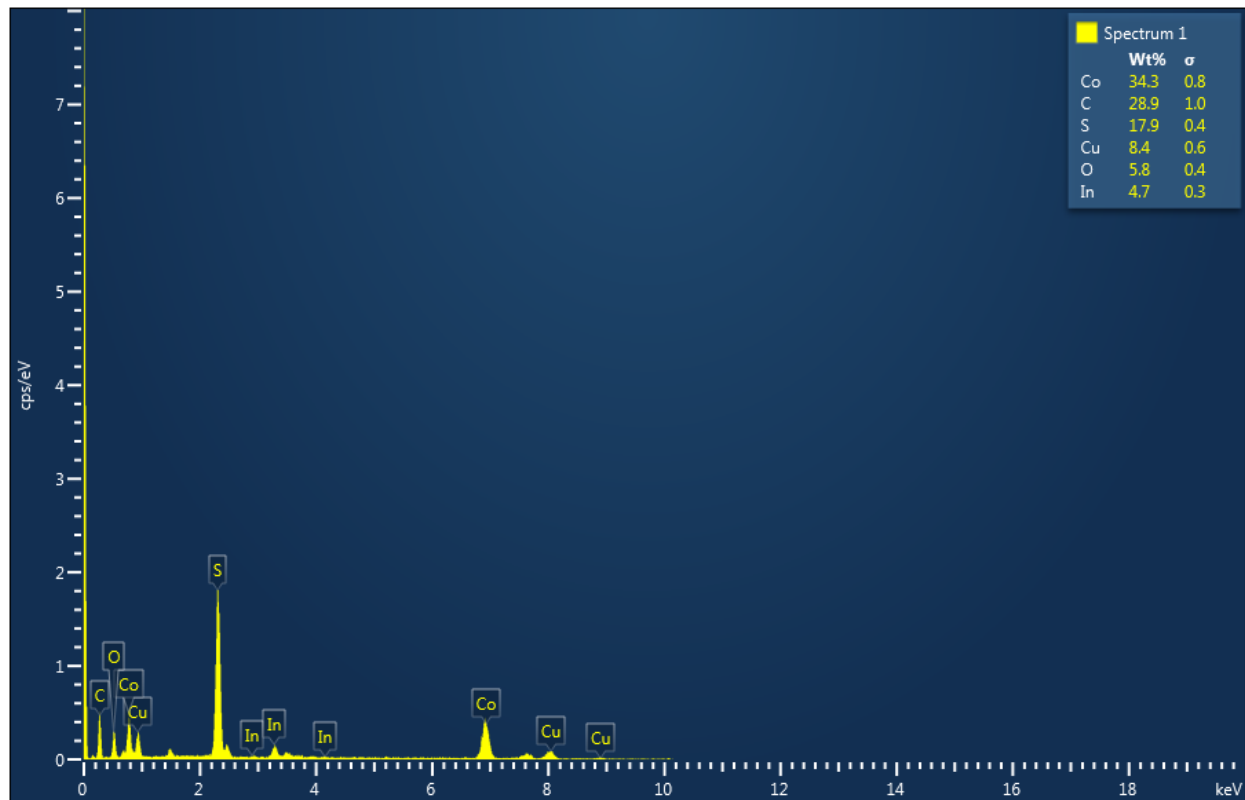


**Figure S2.** EDS profile of CuCo<sub>2</sub>S<sub>4</sub>/g-C<sub>3</sub>N<sub>4</sub>/In<sub>2</sub>S<sub>3</sub> photocatalyst.



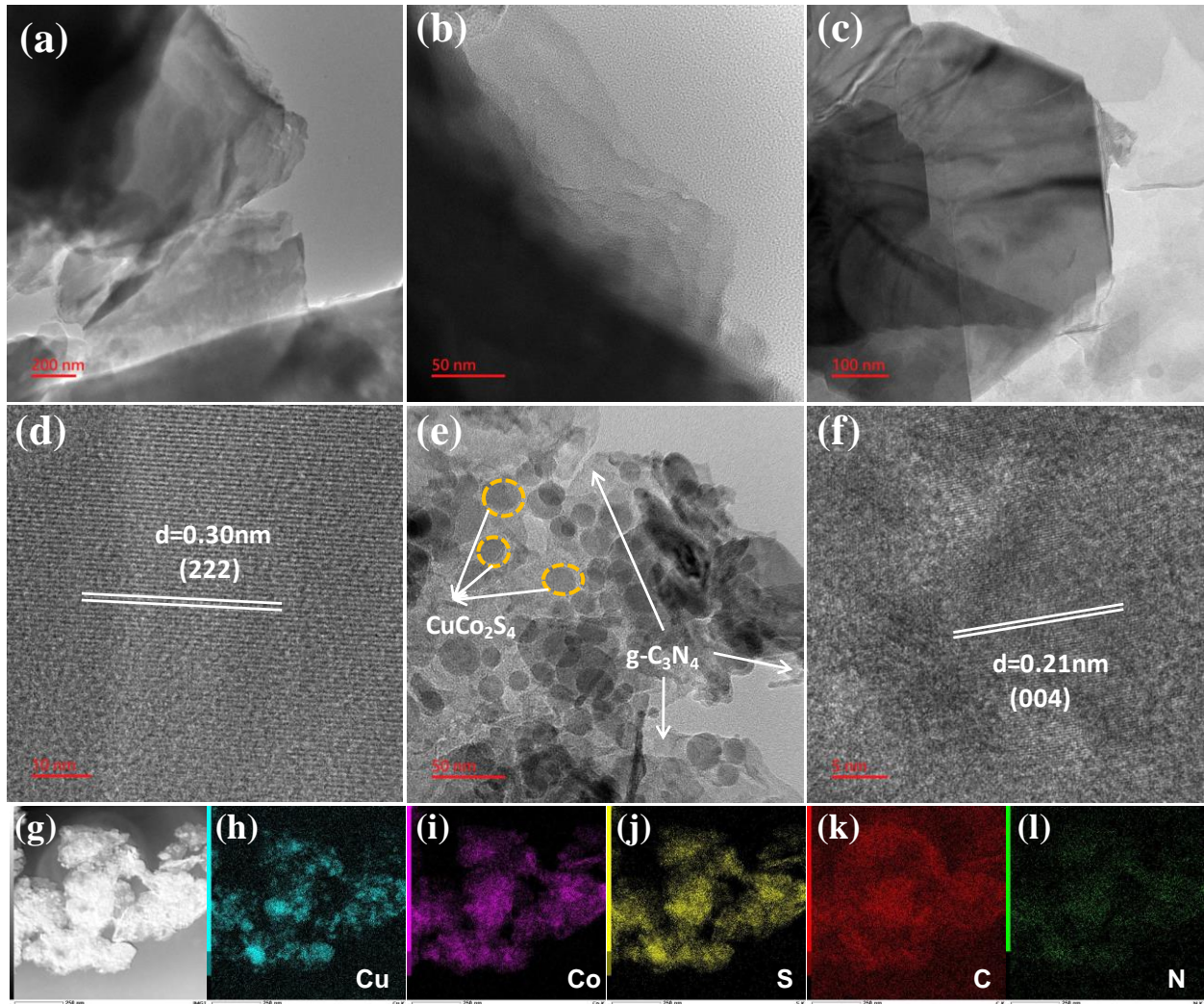


**Figure S3.** TEM Images: (a, b) g-C<sub>3</sub>N<sub>4</sub>, (c, d) In<sub>2</sub>S<sub>3</sub>, (e, f) CuCo<sub>2</sub>S<sub>4</sub>/g-C<sub>3</sub>N<sub>4</sub> and (g-l) elemental mapping of Cu, Co, S, C, N for CuCo<sub>2</sub>S<sub>4</sub>/g-C<sub>3</sub>N<sub>4</sub>.

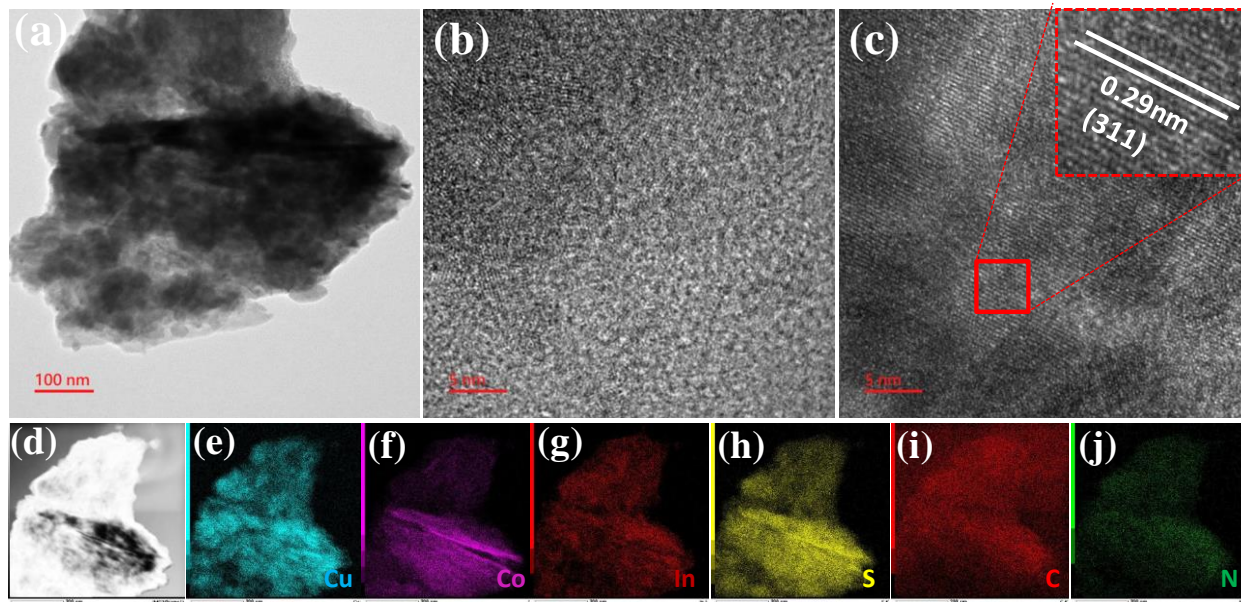


**Figure S4.** TEM Images of  $\text{CuCo}_2\text{S}_4/\text{g-C}_3\text{N}_4/\text{In}_2\text{S}_3$  after photocatalytic analysis and elemental mapping of Cu, Co, S, C, N for  $\text{CuCo}_2\text{S}_4/\text{g-C}_3\text{N}_4$  (d-j).

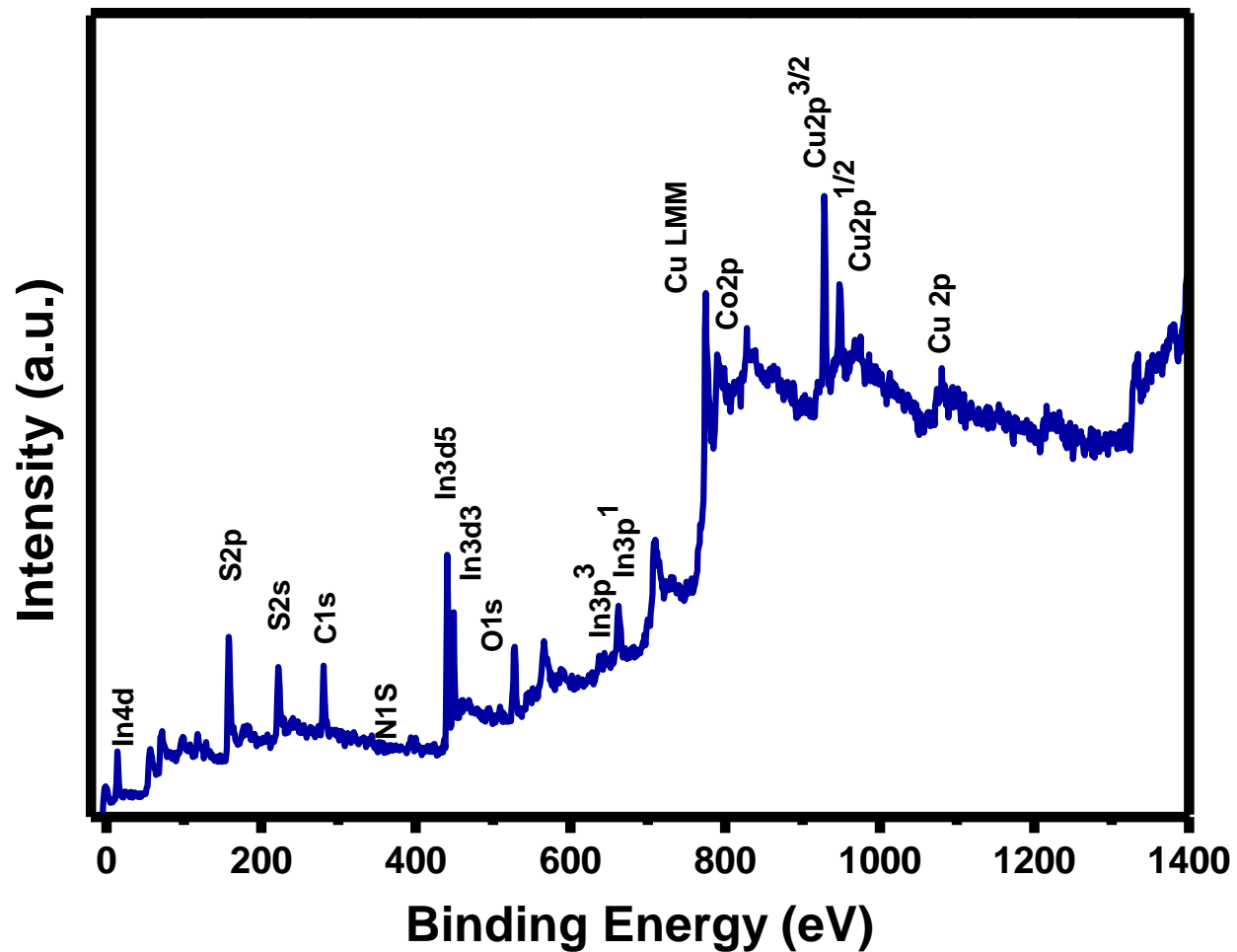
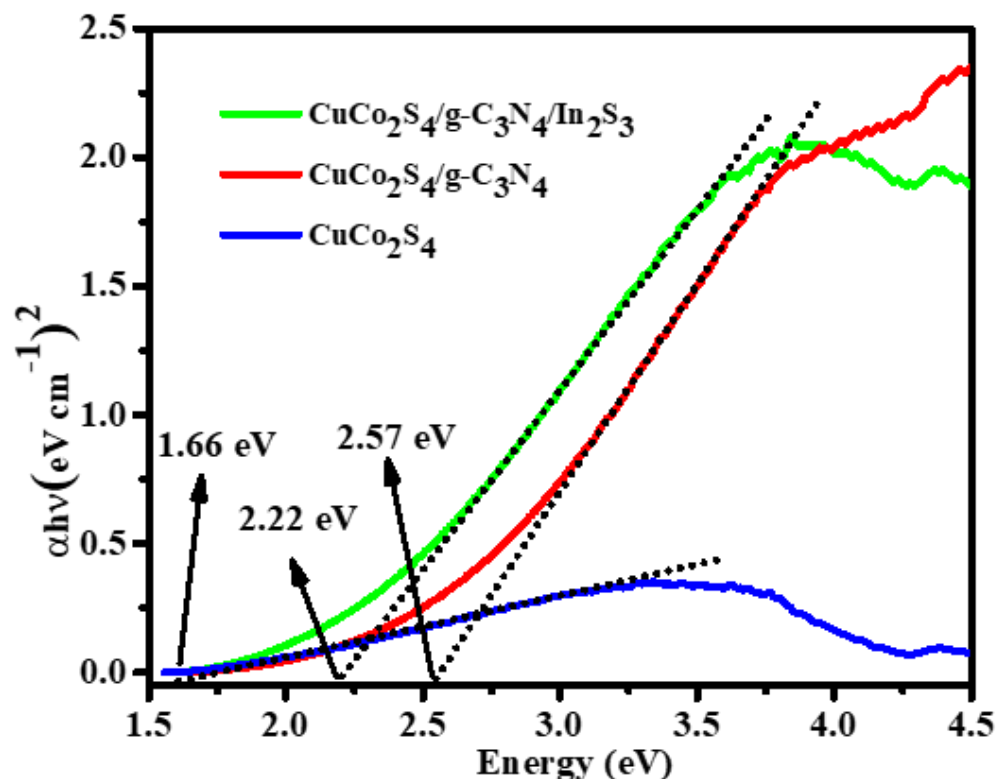


Figure S5. XPS full scan survey spectra of CuCo<sub>2</sub>S<sub>4</sub>/g-C<sub>3</sub>N<sub>4</sub>/In<sub>2</sub>S<sub>3</sub> photocatalyst.



**Figure S6.** Band gap potentials (Tauc plots) of as-synthesized photocatalysts.

## Reference

1. J. P. Perdew, K. Burke and M. Ernzerhof, *Physical Review Letters*, 1996, **77**, 3865-3868.
2. P. E. Blöchl, *Physical Review B*, 1994, **50**, 17953-17979.
3. G. Kresse and J. Furthmüller, *Physical Review B*, 1996, **54**, 11169-11186.
4. H. J. Monkhorst and J. D. Pack, *Physical Review B*, 1976, **13**, 5188-5192.
5. S. Grimme, J. Antony, S. Ehrlich and H. Krieg, *The Journal of Chemical Physics*, 2010, **132**, 154104.
6. J. Heyd and G. E. Scuseria, *The Journal of Chemical Physics*, 2004, **120**, 7274-7280.
7. J. Heyd, G. E. Scuseria and M. Ernzerhof, *The Journal of Chemical Physics*, 2003, **118**, 8207-8215.
8. S. Sk, A. Tiwari, B. M. Abraham, N. Manwar, V. Perupogu and U. Pal, *International Journal of Hydrogen Energy*, 2021, **46**, 27394-27408.
9. S. Sk, C. S. Vennapoosa, A. Tiwari, B. M. Abraham, M. Ahmadipour and U. Pal, *International Journal of Hydrogen Energy*, 2022, **47**, 33955-33965.
10. T.-H. Yu, W.-Y. Cheng, K.-J. Chao and S.-Y. Lu, *Nanoscale*, 2013, **5**, 7356-7360.
11. H. Liu, Z. Xu, Z. Zhang and D. Ao, *Applied Catalysis A: General*, 2016, **518**, 150-157.
12. L. Li, J. Xu, J. Ma, Z. Liu and Y. Li, *Journal of Colloid and Interface Science*, 2019, **552**, 17-26.
13. D. Zhang, Y. Tang, X. Qiu, J. Yin, C. Su and X. Pu, *Journal of Alloys and Compounds*, 2020, **845**, 155569.
14. K. Chang, Z. Mei, T. Wang, Q. Kang, S. Ouyang and J. Ye, *ACS Nano*, 2014, **8**, 7078-7087.
15. Y.-J. Yuan, D. Chen, S. Yang, L.-X. Yang, J.-J. Wang, D. Cao, W. Tu, Z.-T. Yu and Z.-G. Zou, *Journal of Materials Chemistry A*, 2017, **5**, 21205-21213.